Evolution of Multi-Enzyme Complexes: The Case of Tryptophan Synthase†

Sonja Leopoldseder,‡,§ Stefan Hettwer,§,|| and Reinhard Sterner*,‡,§

Institute of Biophysics and Physical Biochemistry, University of Regensburg, Universitätsstrasse 31, D-93053 Regensburg, Germany, and Institute of Biochemistry, University of Cologne, Otto-Fischer-Strasse 12-14, D-50674 Cologne, Germany

Received August 18, 2006; Revised Manuscript Received September 26, 2006

ABSTRACT: The prototypical tryptophan synthase is a stable heterotetrameric α−ββ−α complex. The constituting TrpA and TrpB1 subunits, which are encoded by neighboring genes in the *trp* operon, activate each other in a bi-directional manner. Recently, a novel class of TrpB2 proteins has been identified, whose members contain additional amino acids that might sterically prevent complex formation with TrpA. To test this hypothesis, we characterized the TrpA and TrpB proteins from *Sulfolobus solfataricus*. This hyperthermophilic archaeon does not contain a TrpB1 protein but instead contains two TrpB2 homologues that are encoded within (TrpB2i) and outside (TrpB2o) the *trp* operon. We find that TrpB2i and TrpA form a weak and transient complex during catalysis, with a uni-directional activation of TrpA by TrpB2i. In contrast, TrpB2o and TrpA do not form a detectable complex. These results suggest a model for the evolution of the tryptophan synthase in which TrpB2o, TrpB2i, and TrpB1 reflect the stepwise increase of TrpB affinity for TrpA and the refinement of functional subunit interaction, concomitant with the co-localization of the encoding genes in the *trp* operon.

Multi-enzyme complexes are used by cells to catalyze successive reactions within a metabolic pathway. This allows the organism to coordinate the catalytic activities of the associated subunits and to protect metabolites by direct transfer from one active site to another without being released into the cytoplasm (*1*−*3*). One of the best studied metabolic pathways is the biosynthesis of tryptophan, whose investigation has provided fundamental insights into many aspects of bacterial genetics and enzymology (*4*, *5*). The first and the last steps of tryptophan biosynthesis are catalyzed by multi-enzyme complexes, namely anthranilate synthase and tryptophan synthase. Whereas detailed insights into the structure and mechanism of action of the anthranilate synthase complex were obtained only recently (*6*−*9*), tryptophan synthase has been studied for decades as a model system used to understand the structural basis and functional consequences of protein−protein interactions (*10*).

The prototypical tryptophan synthase found in the mesophilic bacteria *Salmonella typhimurium* and *Escherichia coli* is a α−ββ−α complex (*11*), whose α- and β-subunits are encoded in the tryptophan operon by the adjacent *trp*A and *trp*B1 genes. TrpA catalyzes the reversible cleavage of indole-3-glycerol phosphate (IGP[1]) into glyceraldehyde-3-phosphate (GA3P) and indole (reaction 1). The indole migrates through a hydrophobic channel to an active site of an attached TrpB1 subunit (*12*), where it condenses with L-serine in a pyridoxal phosphate (PLP) dependent irreversible reaction to form L-tryptophan (reaction 2). The physiologically relevant reaction of the α−ββ−α complex is the sum of the TrpA and TrpB1 reactions (reaction 3).

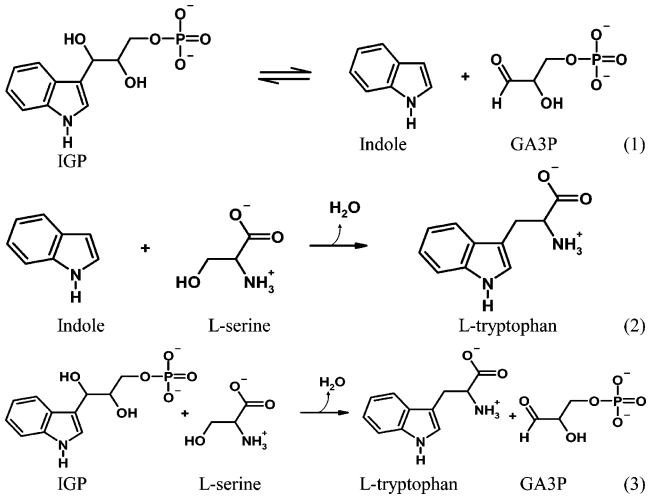

The catalytically essential residues of the α- and β-subunits have been identified, and their reaction mechanisms have been elucidated (*13*, *14*). The isolated TrpA and TrpB proteins form stable but poorly active α-monomers (*15*) and ββ-homodimers (*16*) with molecular masses of about 27 and 94 kDa, respectively. Their assembly to the native α-ββ-α

† S.L. was supported by a Ph.D. fellowship from the *Fonds der Chemischen Industrie*.

* Corresponding author. Phone: +49-941-943 3015. Fax: +49-941-943 2813. E-mail: reinhard.sterner@biologie.uni-regensburg.de.

‡ University of Regensburg.

§ University of Cologne.

|| Present address: Department of Biochemistry, University of Zurich, Winterthurer Strasse 190, CH-8057 Zurich, Switzerland.

[1] Abbreviations: GA3P, glyceraldehyde-3-phosphate; IGP, indole-3-glycerol phosphate; PLP, pyridoxal phosphate; TrpA, α-subunit of tryptophan synthase; sTrpA, TrpA from *Sulfolobus solfataricus*; tmTrpA, TrpA from *Thermotoga maritima*; TrpB, β-subunit of tryptophan synthase; sTrpB2i/sTrpB2o, TrpB variants from *Sulfolobus solfataricus*; tmTrpB1/tmTrpB2, TrpB variants from *Thermotoga maritima*.

10.1021/bi061684b CCC: $33.50
Published on Web 11/04/2006

complex, however, leads to structural alterations of both subunit types (*17*), which results in their reciprocal activation by 1−2 orders of magnitude (*18*). This inter-subunit communication is based on conformational transitions between open (catalytically inactive) and closed (catalytically active) states (*19*), whose equilibrium can be shifted by α-subunit ligands, monovalent cations, solvents, temperature, or pressure (ref 20 (*20*) and references therein). The ligand-induced structural changes between the various states and the residues crucial for the allosteric communication between the α- and *β*-active sites were identified by X-ray crystallography, NMR spectroscopy, and mutational analysis of the *S. typhimurium* tryptophan synthase (*21*−*31*).

These findings establish that the α- and *β*-subunits of tryptophan synthase are highly interactive, both with respect to structure and function. It was, therefore, unexpected when whole genome sequencing identified two different *trp*B genes (*trp*B1 and *trp*B2) but only a single *trp*A gene in many Archaea and a few Bacteria and plants. The TrpB1 and TrpB2 proteins constitute two phylogenetically distinct sequence families (*32*), which are listed in the clusters of orthologous groups of proteins database (*33*) as COG 0133 and 1350, respectively. Within each of the two groups, proteins show sequence identities of about 60%, whereas between the two groups, the identities are only about 30% (*34*). Most *trp*B1 genes, which correspond to the conventional *trp*B genes, are localized in the *trp* operon adjacent to *trp*A. In contrast, most *trp*B2 genes are located outside this operon.

Recently, tmTrpA, tmTrpB1, and tmTrpB2 from the hyperthermophilic bacterium *Thermotoga maritima* (optimum growth at 80 °C) were produced in *E. coli*, purified, and characterized (*34*). It was shown that recombinant tmTrpA forms an α-monomer and that both recombinant tmTrpB proteins form *ββ*-homodimers. However, only the operon-encoded tmTrpB1 but not tmTrpB2 associates with tmTrpA to form the conventional α−*ββ*−α tryptophan synthase complex in which both subunits reciprocally activate each other. Compared to tmTrpB1, tmTrpB2 and all other identified TrpB2 proteins contain an *N*-terminal extension of about 20 residues and 2 insertions in the communication (*COMM*) domain of about 5 and 10 residues, and it was postulated that these additional residues prevent complex formation with TrpA by steric hindrance (*34*) (Figure 1).

Sulfolobus solfataricus is a hyperthermophilic crenarchaeon, which grows optimally at temperatures between 75 and 80 °C and at pH values between 2 and 4 (*35*). In contrast to *T. maritima*, the genome of *S. solfataricus* does not contain a *trp*B1 gene but has two different *trp*B2 genes, s*trp*B2i and s*trp*B2o, as defined by the COG database (*35*) (Figure 1). Whereas s*trp*B2i is located next to s*trp*A within the *trp* operon, s*trp*B2o is located more than 20 kbp outside the operon. The same situation is found in four other crenarchaea (*S. tokodaii*, *Aeropyrum pernix*, *Pyrobaculum aerophilum*, and *Picrophilus torridus*) (*36*−*39*). Following the hypothesis that TrpB2 proteins do not form a complex with TrpA (*34*), one would have to conclude that these five microorganisms do not contain a prototypical tryptophan synthase α−*ββ*−α complex and, as a consequence, lack the sophisticated system of mutual subunit activation and indole channelling described above.

In order to test this hypothesis, we have produced sTrpA, sTrpB2i, and sTrpB2o in *E. coli* and purified and characterized the recombinant proteins. The results show that sTrpB2i, but not sTrpB2o, associates transiently with sTrpA during catalysis to form a functional tryptophan synthase complex. However, in contrast to the regular tryptophan synthases, activation is uni-directional from sTrpB2i to sTrpA, and the affinity between the different subunit types is weak. On the basis of these findings, we propose a model for the evolution of the tryptophan synthase which might be paradigmatic for other key metabolic enzyme complexes.

MATERIALS AND METHODS

DNA Manipulation and Sequence Analysis. Preparation of DNA, digestion with restriction endonucleases, ligation, and sequencing of DNA were performed as described (*40*). DNA amplification by PCR was performed using the Ready-MixREDTaq PCR Reaction Mix (Sigma-Aldrich) or the Pwo Polymerase (New England Biolabs).

Gene Cloning and Protein Production. The s*trp*A, s*trp*B2i, and s*trp*B2o genes, as well as the genes for glyceraldehyde-3-phosphate dehydrogenase (tm*gapdh*) and lactate dehydrogenase (tm*ldh*) from *T. maritima* were subcloned into the pET28a vector (Stratagene), and expressed in *E. coli* BL21-(DE3) Codon plus cells. The recombinant proteins were purified from the soluble fraction of the cell extract using a heat step to remove thermolabile host proteins, followed by metal chelate affinity chromatography. In the case of sTrpA, sTrpB2i, and sTrpB2o, the *N*-terminal His-tag was cleaved by thrombin and removed together with the protease by hydroxyapatite or anion exchange chromatography. The details of the protocols for cloning, heterologous expression, and purification are provided in Supporting Information. The tmTrpA and tmTrpB1 proteins were produced by heterologous gene expression in *E. coli* and purified as described (*34*).

Analytical Methods. Purification of proteins was followed by electrophoresis on 12.5% SDS-polyacrylamide gels with the system of Laemmli (*41*) using staining with Coomassie blue. The concentrations of sTrpA, tmGAPDH, and tmLDH were determined using the molar extinction coefficients at 280 nm calculated from the amino acid sequences (*42*): $\epsilon_{280} = 25900\ M^{-1}\ cm^{-1}$ for sTrpA, $\epsilon_{280} = 24410\ M^{-1}\ cm^{-1}$ for tmGAPDH, and $\epsilon_{280} = 18910\ M^{-1}\ cm^{-1}$ for tmLDH. The concentrations of sTrpB2i and sTrpB2o were measured according to the Bradford procedure (*43*) because the strong absorption at 280 nm of the bound cofactor PLP impeded a reliable calculation of ϵ_{280}. Analytical gel filtration was performed at 25 °C and a flow rate of 0.5 mL min^{-1} on a Superdex 200 column (GE Healthcare) equilibrated with 50 mM potassium phosphate buffer at pH 7.5, containing 300 mM KCl. Apparent molecular masses were calculated from the corresponding elution volumes using a calibration curve that was obtained with standard proteins. Sedimentation equilibrium runs with 4 *μ*M (subunit concentration) sTrpB2i or sTrpB2o were performed at 26.5 °C in a Beckman analytical ultracentrifuge (model E) at 12000 rpm and followed by measuring the absorbance at 277 nm. The proteins were dissolved in 10 mM potassium phosphate buffer at pH 7.5, containing 40 *μ*M PLP. The runs were analyzed using the meniscus-depletion-method (*44*, *45*).

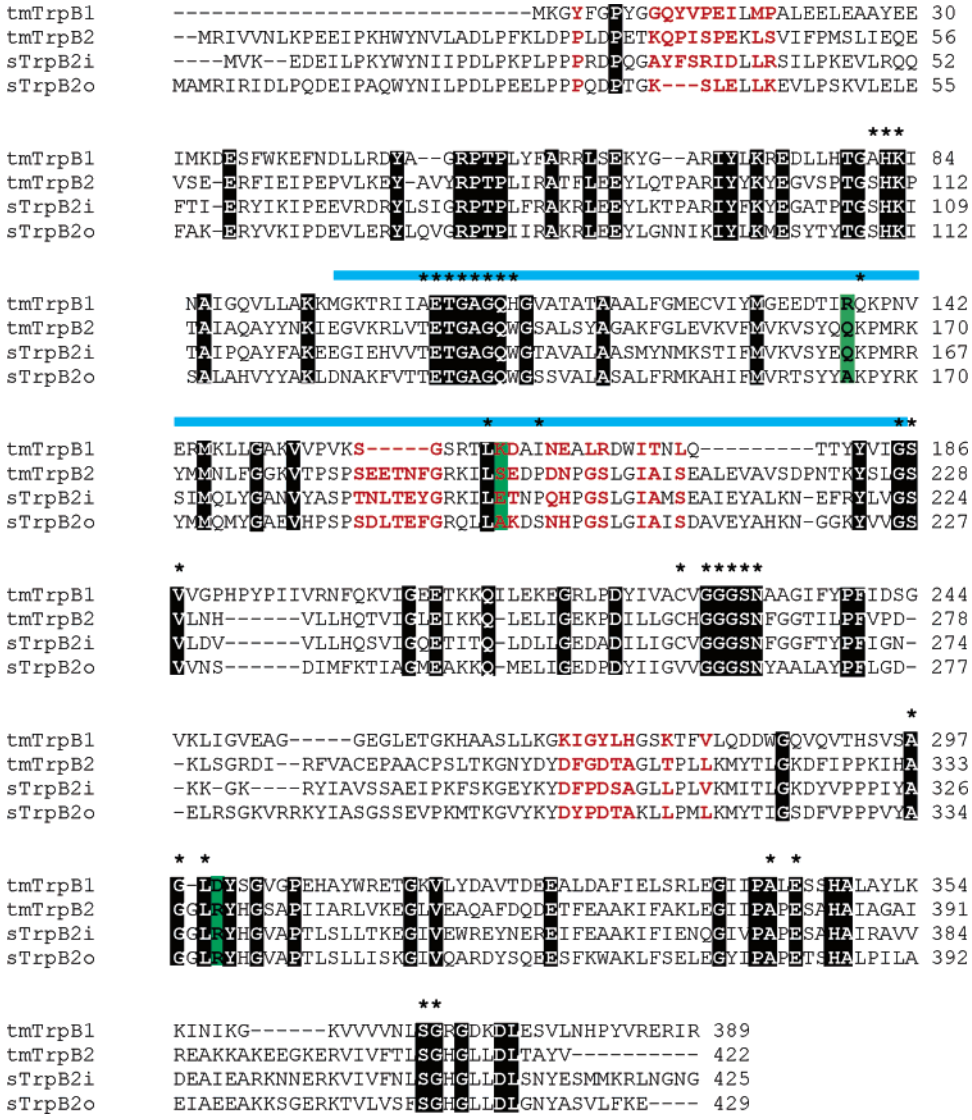

FIGURE 1: Multiple sequence alignment of the tryptophan synthase β-subunits from *T. maritima* and *S. solfataricus*. Amino acids conserved in the four sequences are displayed in black columns; *, amino acids at a distance of 4 Å or less from the bound tryptophan in TrpB1 from *S. typhimurium* (pdb code 2TYS). The blue bars mark the residues of the communication (*COMM*) domain (*23*). It has been postulated that the insertions in *COMM* domains of tmTrpB2 and its *N*-terminal extension prevent complex formation with tmTrpA (*34*). The amino acids in red are at a distance of 5 Å or less from TrpA in TrpB1 from *S. typhimurium* (pdb code 1A50). The amino acids in green columns are conserved in the known TrpB1 sequences (R137, K163, D300 in tmTrpB1) but not in the TrpB2 sequences. They form intra and intersubunit salt bridges, which are involved in the allosteric communication between TrpA and TrpB1 (*28*). The alignment was created with T-coffee (*61*).

Molecular masses were calculated assuming a partial specific volume of 0.73 mL/g.

Steady-State Enzyme Kinetics. The cleavage of IGP to indole and GA3P (A-reaction) by sTrpA or tmTrpA was measured at 60 °C by absorption spectroscopy in a coupled enzymatic assay (*46*) and analyzed using $\Delta\epsilon_{340}$(NADH − NAD$^+$) = 6.22 mM^{-1} cm^{-1} as described (*34*). Initial velocity measurements were recorded in 100 mM EPPS/KOH buffer at pH 7.5, containing 180 mM KCl, 40 μM PLP, 6 mM NAD$^+$, 20 mM arsenate, 5.5 μM tmGAPDH, and various concentrations of IGP. The values for the steady-state enzyme kinetic parameters k_{cat} and K_M^{IGP} were determined by the fitting of saturation curves with a hyperbolic function.

For the generation of Arrhenius diagrams, the turnover numbers of sTrpA and tmTrpA were determined at saturating concentrations of IGP. The applied concentrations for isolated sTrpA were 10 μM at 55 °C, 15 μM at 50 and 60 °C, and 27 μM at 45 °C. The concentration of isolated tmTrpA was 8 μM for the entire temperature range between 30 and 60 °C. At the same temperatures as those applied to the isolated TrpA proteins, 3 μM sTrpA was assayed in the presence of 0.5 μM (subunit concentration) sTrpB2i plus 1 M serine, and 1 μM tmTrpA was assayed in the presence of 1 μM (subunit concentration) tmTrpB1 plus 1 M serine.

The conversion of indole and serine to tryptophan (B-reaction) by sTrpB2i and sTrpB2o was measured at 60 °C by absorption spectroscopy and analyzed using $\Delta\epsilon_{290}$ (tryptophan − indole) = 1.89 mM^{-1}cm^{-1} (*47*). Initial velocity measurements in the presence of saturating concentrations of indole and various concentrations of serine were recorded in 100 mM potassium phosphate buffer at pH 7.5, containing 180 mM KCl and 40 μM PLP. The values for the steady-state enzyme kinetic parameters k_{cat} and K_M^{serine} were determined by the fitting of saturation curves with a hyperbolic function. The values for K_M^{indole} were determined by analyzing entire progress curves, which were recorded

in the same buffer in the presence of saturating concentrations of serine, with the integrated form of the Michaelis−Menten equation (*48*).

The cleavage of serine to pyruvate and ammonia (serine deaminase reaction) catalyzed by the TrpB proteins was measured at 80 °C with a coupled spectroscopic assay (*49*) in which the produced pyruvate is converted by tmLDH to lactate, upon the oxidation of NADH to NAD^+. Initial velocity measurements in the presence of various concentrations of serine were recorded in 100 mM potassium phosphate buffer at pH 7.5, containing 180 mM KCl, 40 μM PLP, 250 μM NADH, and 10 μM tmLDH. The values for the steady-state enzyme kinetic parameters k_{cat} and K_M^{serine} were determined by the fitting of saturation curves with a hyperbolic function.

Activity Titrations. sTrpB2i and tmTrpB1 were titrated at 60 °C with sTrpA and tmTrpA, respectively, both in the presence and absence of 1 M serine. The resulting A-activities of the complexed TrpA proteins were measured, corrected for the activities of the isolated TrpA proteins, and normalized. The titrations of sTrpB2i with sTrpA could be fitted with a hyperbolic function. The titrations of tmTrpB1 with tmTrpA, however, yielded a linear graph almost until saturation was reached, indicating that the free concentration of tmTrpA was much lower than its added total concentration. For this reason, the curves were fitted with the following quadratic equation:

$$[PL]_{eq}/[P_0] = 1/2(d - \sqrt{d^2 - 4c}) \qquad (1)$$

where $d = 1 + ([L]_0 + K_d)/([P]_0)$, and $c = [L]_0/[P]_0$.

$[PL]_{eq}$ is the equilibrium concentration of the complex between tmTrpB1 and tmTrpA, $[P_0]$ is the total concentration of tmTrpB1, and $[L]_0$ is the total concentration of tmTrpA.

RESULTS

Association States and Test for Complex Formation of sTrpA with sTrpB2i and sTrpB2o. To investigate the association states of the recombinant proteins and to test whether sTrpA forms a complex with sTrpB2i or sTrpB2o, analytical gel filtration was performed at 25 °C on a calibrated superdex 200 column. The results are presented in Figure 2. The elution profiles of the protein mixtures correspond to the sum of the elution profiles of the individual proteins, demonstrating that sTrpA does not form a stable complex with either sTrpB2i or sTrpB2o under the given conditions. Likewise, the elution profile of a mixture of tmTrpA and tmTrpB2 corresponded to the sum of the elution profiles of the separated proteins, whereas a mixture of tmTrpA and tmTrpB1 yielded a faster eluting peak, corresponding to the α−ββ−α complex (*34*).

The elution time of sTrpA corresponds to a molecular mass of 25.5 kDa, matching within experimental error the calculated molecular mass for the monomer of 27.9 kDa. The elution times of sTrpB2i and sTrpB2o correspond to molecular masses of 55.7 and 83.5 kDa, respectively, which are between the calculated molecular masses of the respective β-monomers (47.7 and 47.8 kDa) and ββ-homodimers (95.4 and 95.6 kDa). Sedimentation equilibrium runs in the analytical ultracentrifuge yielded molecular masses of 92.0 kDa for sTrpB2i and 104.0 kDa for sTrpB2o, confirming that both proteins are homodimers.

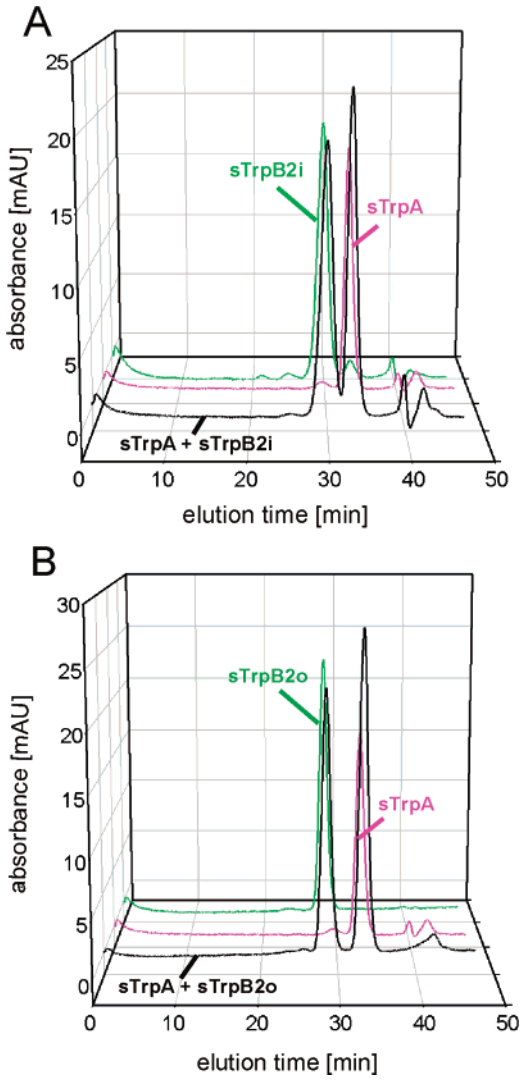

FIGURE 2: Analytical gel filtration at 25 °C to test for stable complex formation between sTrpA and sTrpB2i (A) or sTrpB2o (B). (A) Elution profiles of 12 μM sTrpA (magenta), 6 μM (subunit concentration) sTrpB2i (green), and a 1:1 mixture of the two protein solutions (black). (B) Elution profiles of 12 μM sTrpA (magenta), 6 μM (subunit concentration) sTrpB2o (green), and a 1:1 mixture of the two protein solutions (black). The elution was performed at a flow rate of 0.5 mL/min in 50 mM potassium phosphate buffer at pH 7.5 and 300 mM KCl and was followed by measuring the absorbance at 280 nm.

Catalytic Activities of sTrpA and tmTrpA. Analytical gel filtration at 25 °C did not provide evidence for the formation of a stable complex between sTrpA and sTrpB2i or sTrpB2o (Figure 2). To test whether complex formation is induced by temperatures close to the growth optimum of *S. solfataricus* or by the presence of substrates, the stimulation of sTrpA activity by sTrpB2i or sTrpB2o was assayed by steady-state enzyme kinetics at 60 °C with and without serine. For comparison, the stimulation of tmTrpA by tmTrpB1 in the $[tmTrpA-tmTrpB1]_2$ complex was measured under identical conditions. The deduced values for the turnover numbers k_{cat}, Michaelis constants K_M^{IGP}, and catalytic efficiencies k_{cat}/K_M^{IGP} are listed in Table 1. The data show that sTrpB2o, even when present at high concentrations, does not increase the poor catalytic activity of sTrpA.

Table 1: Steady-State Enzyme Kinetic Parameters at 60 °C of sTrpA and tmTrpA, in the Absence and Presence of the Cognate TrpB Proteins and Serine[a]

protein	k_{cat} (s^{-1})	K_M^{IGP} (mM)	k_{cat}/K_M^{IGP} ($mM^{-1}\,s^{-1}$)
sTrpA[b]	0.0007	0.012	0.058
sTrpA + sTrpB2i[c]	0.012	0.0035	3.4
ratio[d]	*17*	*0.29*	*59*
sTrpA + sTrpB2i + serine[e]	0.10	0.0062	16
ratio[d]	*143*	*0.52*	*275*
sTrpA + sTrpB2o[f]	0.0007	0.012	0.058
ratio[d]	*1*	*1*	*1*
tmTrpA[g]	0.052	0.65	0.08
$[tmTrpA-tmTrpB1]_2$[h]	0.52	0.11	4.7
ratio [d]	*10*	*0.17*	*59*
$[tmTrpA-tmTrpB1]_2$ + serine[i]	1.1	0.013	85
ratio[d]	*21*	*0.02*	*1050*

[a] Reaction conditions: 100 mM EPPS/KOH at pH 7.5, 180 mM KCl, 40 μM PLP, 6 mM NAD^+, and 5.5 μM tmGAPDH. [b] 14 μM sTrpA. [c] 3 μM sTrpA plus 0.5 μM (subunit concentration) sTrpB2i. [d] Ratio of the values for the TrpA proteins in the presence and absence of the cognate TrpB proteins (and serine, if applicable). [e] 3 μM sTrpA plus 0.5 μM (subunit concentration) sTrpB2i plus 1 M serine. [f] 14 μM sTrpA plus 28 μM (subunit concentration) sTrpB2o. [g] 8 μM tmTrpA. [h] 1 μM $[tmTrpA-tmTrpB1]_2$. [i] 1 μM $[tmTrpA-tmTrpB1]_2$ plus 0.5 M serine. The measurements were made in duplicate, and the values of the determined constants deviated by less than 30%.

In contrast, sTrpB2i increases the catalytic efficiency k_{cat}/K_M^{IGP} of sTrpA about 60-fold because of a strong increase of k_{cat} and a moderate decrease of K_M^{IGP}. When the sTrpB2i substrate serine is present at saturating concentrations, sTrpA is activated almost 300-fold. These results demonstrate that sTrpA and sTrpB2i form a productive complex during catalysis at 60 °C and that the binding of serine further enhances the stimulating effect of sTrpB2i for sTrpA. Likewise, isolated tmTrpA shows a low catalytic efficiency at 60 °C and is stimulated by tmTrpB1 about 60-fold in the absence and more than 1000-fold in the presence of serine (Table 1).

Temperature Dependence of the Activation of sTrpA and tmTrpA by Their Cognate TrpB Proteins. Although no complex between sTrpA and sTrpB2i was detected by analytical gel filtration at 25 °C, the catalytic efficiency of sTrpA was greatly increased by sTrpB2i at 60 °C (Table 1). These findings suggested that high temperature is required for productive interactions between sTrpA and sTrpB2i but might be less important for interactions between tmTrpA and tmTrpB1, which form a stable complex that is detectable by analytical gel filtration at 25 °C (*34*). To test this hypothesis, the activation of sTrpA and tmTrpA by their cognate sTrpB2i and tmTrpB1 proteins was assayed at a temperature range between 30 and 60 °C. The results are presented in Figure 3. The Arrhenius diagrams in both Figure 3A and B are parallel to a first approximation, demonstrating that the activation of both sTrpA by sTrpB2i and tmTrpA by tmTrpB1 is largely independent of temperature.

Monitoring Complex Formation by Activity Titrations. To test whether a low affinity of sTrpA for sTrpB2i might prevent the detection of a stable complex, titration studies were performed. To this end, constant concentrations of sTrpB2i and tmTrpB1 were supplemented with increasing amounts of sTrpA and tmTrpA, respectively, and the formation of complexes was assayed by measuring the activation of TrpA when bound to the cognate TrpB. The

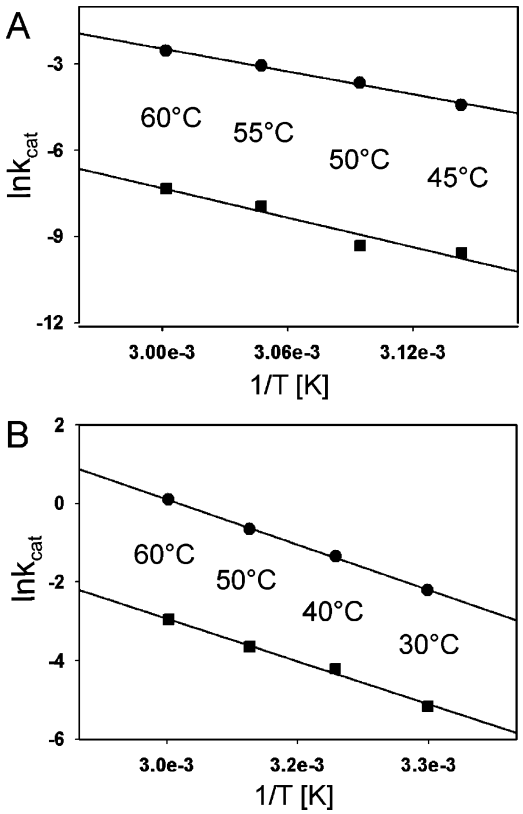

FIGURE 3: Temperature dependence of the activation of sTrpA by sTrpB2i (A) and tmTrpA by tmTrpB1 (B) (Arrhenius diagrams). The turnover numbers of sTrpA (A) and tmTrpA (B) were measured in the absence (■) and presence (●) of saturating concentrations of sTrpB2i and tmTrpB1, respectively, plus 1 M serine. The deduced activation energies for isolated and complexed sTrpA are 142 and 123 kJ/mol, and those for isolated and complexed tmTrpA are 60 and 63 kJ/mol, respectively.

results are shown in Figure 4. The activation of sTrpA with sTrpB2i with bound serine was fitted with a hyperbolic function, yielding an apparent K_d value for complex formation of 0.28 μM. The activation of tmTrpA by tmTrpB1 with bound serine is linear over almost the entire applied concentration range, and the extrapolated equivalence point of 0.06 μM tmTrpA at the given tmTrpB1 subunit concentration of 0.05 μM confirmed the 1:1 stoichiometry in the $[tmTrpA-tmTrpB1]_2$ complex (*34*). The curve was fitted with a quadratic equation (Material and Methods) (*50*), yielding an apparent K_d value of ~0.4 nM. This value is close to the K_d value of 2 nM, which was determined at 25 °C in a similar way for the formation of the $\alpha-\beta\beta-\alpha$ complex from *E. coli* (*51*). These findings show that complex formation between sTrpA and sTrpB2i takes place with an affinity that is lower by almost 3 orders of magnitude in comparison to the affinity between TrpA and TrpB1 proteins. The apparent affinity between tmTrpA and tmTrpB1 is independent of the presence of serine within experimental error. In contrast, the apparent affinity between sTrpA and sTrpB2i is decreased 100-fold in the absence of serine, yielding an apparent K_d value of 22 μM (Figure 4). These results suggest that the activating effect of serine (Table 1) is due to an improved functional coupling between tmTrpB1 and tmTrpA and an increased affinity of sTrpB2i for sTrpA.

Catalytic Activities of sTrpB2i and sTrpB2o. Steady-state enzyme kinetics with sTrpB2i and sTrpB2o were measured at 60 °C, both in the absence and in the presence of sTrpA.

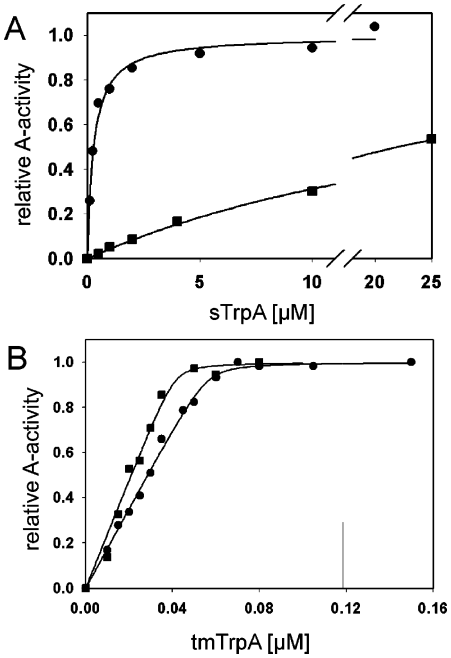

FIGURE 4: Activity titration studies to quantify the binding of sTrpA to sTrpB2i (A) and tmTrpA to tmTrpB1 (B). (A) 0.5 μM (subunit concentration) sTrpB2i and (B) 0.05 μM (subunit concentration) tmTrpB1 were titrated at 60 °C with the indicated concentrations of sTrpA and tmTrpA, respectively. The measured activities of complexed TrpA in the presence of 1 mM IGP were corrected for the low activities of the isolated proteins (see Table 1) and normalized. The titrations were performed in the absence (■) and the presence (●) of 1 M serine. The lines show the results of fits of the curves with (A) a hyperbolic function, yielding apparent K_d values of 0.28 μM (with serine) and 22 μM (without serine) and (B) a quadratic function (eq 1), yielding apparent K_d values of ~0.3 nM (without serine) and 0.4 nM (with serine).

Table 2: Steady-State Enzyme Kinetic Parameters at 60 °C of sTrpB2i and sTrpB2o, in the Absence and Presence of sTrpA[a]

protein	k_{cat} (s^{-1})	K_M^{indole} (μM)	k_{cat}/K_M^{indole} ($\mu M^{-1} s^{-1}$)	K_M^{serine} (M)	k_{cat}/K_M^{serine} ($M^{-1} s^{-1}$)
sTrpB2i[b]	0.20	3	0.067	0.035	5.7
sTrpB2i + sTrpA[b]	0.18	6	0.030	0.046	3.9
sTrpB2o[c]	0.032	6	0.0053	0.151	0.21
sTrpB2o + sTrpA[c]	0.033	8	0.0041	0.070	0.47

[a] Reaction conditions: 100 mM potassium phosphate at pH 7.5, 180 mM KCl, and 40 μM PLP. [b] 0.76 μM (subunit concentration) sTrpB2i ± 1.5 μM sTrpA. [c] 4 μM (subunit concentration) sTrpB2o ± 8 μM sTrpA. The measurements were made in duplicate, and the values of the determined constants deviated by less than 30%.

The deduced values for k_{cat}, K_M^{indole}, K_M^{serine}, k_{cat}/K_M^{indole}, and k_{cat}/K_M^{serine} are listed in Table 2. The catalytic efficiencies of sTrpB2i for indole and serine are about 1 order of magnitude higher than those of sTrpB2o, mainly because of an increased k_{cat} value. However, neither sTrpB2 protein is activated by sTrpA. Given the lack of activation of sTrpA by sTrpB2o (Table 1), this result is in accordance with expectations. It is unexpected, however, in the case of sTrpB2i, which strongly activates sTrpA (Table 1; Figure 3A).

Serine Deaminase Activity of TrpB Proteins. It has been suggested that TrpB2 enzymes might act as indole salvage proteins, which prevent the diffusion of the hydrophobic metabolite through the cell membrane at the high physiological temperatures of hyperthermophiles (*34*). Alternatively, it has been proposed that the deamination of serine to pyruvate is the physiological function of TrpB2 proteins. In support of this hypothesis, serine deamination is a known side reaction of TrpB1 proteins (*49*) and almost all organisms with a *trp*B2 gene, including *T. maritima* and *S. solfataricus*, lack a serine deaminase gene (*32*). Along the same lines, it has been speculated that the expression of *trp*B2 from *Methanothermobacter thermautotrophicus* might be regulated by the availability of serine (*52*). To follow up the serine deaminase hypothesis, the cleavage of serine to pyruvate and ammonia by sTrpB2o and tmTrpB2 was measured at 80 °C. Both sTrpB2o and tmTrpB2 showed poor serine deaminase activities with catalytic efficiencies k_{cat}/K_M^{serine} of 0.9 M^{-1} s^{-1} (k_{cat} = 0.036 s^{-1}, K_M^{serine} = 0.042 M) and 1.4 M^{-1} s^{-1} (k_{cat} = 0.010 s^{-1}, K_M^{serine} = 0.007 M), respectively. These values are lower by 1−2 orders of magnitude than the corresponding k_{cat}/K_M^{serine} values of tmTrpB1 and [tmTrpA−tmTrpB1]$_2$, which were determined to be 13 M^{-1} s^{-1} (k_{cat} = 0.63 s^{-1}, K_M^{serine} = 0.047 M) and 340 M^{-1} s^{-1} (k_{cat} = 0.29 s^{-1}, K_M^{serine} = 0.00086 M), respectively. These findings do not support the assumption that serine deamination is the main function of sTrpB2o or tmTrpB2 *in vivo*.

DISCUSSION

Complex Formation between sTrpB2i and sTrpA. The sequence alignment depicted in Figure 1 shows that the main deviations of TrpB2 from TrpB1 proteins are an *N*-terminal extension and two insertions in the *COMM* domain (*23*). It has been postulated that these additional sequence stretches in TrpB2 prevent complex formation with TrpA (*34*). Moreover, arginine, lysine, and aspartate residues conserved in TrpB1 sequences and involved in the $\alpha-\beta$ subunit communication within tryptophan synthase complexes are missing in the TrpB2 sequences (Figure 1; (*28*)). Along these lines, no stable complex between sTrpB2i and sTrpA could be detected by analytical gel filtration (Figure 2A) or sedimentation velocity runs in the analytical ultracentrifugation, even in the presence of micromolar concentrations of both proteins (data not shown). Nevertheless, sTrpB2i activates sTrpA in steady-state enzyme kinetic measurements up to 300-fold (Table 1; Figure 3A). Taken together, these findings suggest that complex formation between sTrpA and sTrpB2i is transient and occurs only in the course of catalysis. It will be the subject of future studies to elucidate at which stage of the catalytic cycle the two proteins associate and by which mechanism sTrpA is activated by sTrpB2i.

It is noteworthy that sTrpA is activated by sTrpB2i but not vice versa (Tables 1 and 2). This uni-directional activation is a novel finding because in all previously investigated $\alpha-\beta\beta-\alpha$ tryptophan synthases, the two different subunits mutually stimulate each other (*53*). It is interesting to note, however, that in the complex between sTrpA and sTrpB2i, the turnover number of the A-reaction is still lower (0.10 s^{-1}) by a factor of 2 compared to the turnover number of the B-reaction (0.20 s^{-1}). This result shows that the A-reaction is rate-limiting for the overall turnover and that an activation of sTrpB2i by sTrpA would not further increase the catalytic rate of the *S. solfataricus* tryptophan synthase complex.

Why does sTrpB2i form a transient complex with sTrpA, whereas sTrpB2o does not? The alignment in Figure 1

reveals a short gap in the *N*-terminal region of sTrpB2o, which is filled with the three amino acids Y33, F34, and S35 in sTrpB2i. Model building suggests that these three residues form a tip, which protrudes into sTrpA and forms numerous hydrophobic interactions. Ongoing mutational studies will show whether the deletion of these amino acids from sTrpB2i and their insertion into sTrpB2o will influence complex formation with and activation of sTrpA.

Although the mechanism and the structural basis of the transient interaction between sTrpB2i and sTrpA are yet unclear, it is not unprecedented. The analysis of enzyme kinetic data proved that functional interactions and metabolite channelling take place between the glutaminase (PabA) and synthase (PabB) subunits of *p*-aminobenzoic synthase as well as between glutamine phosphoribosylpyrophosphate amidotransferase (PRPP-AT) and glycinamide ribonucleotide synthetase (GAR-syn). Nevertheless, no stable complexes between PabA and PabB or PRPP-AT and GAR-syn could be detected (*54*, *55*).

Implications for the Evolution of the Tryptophan Synthase Complex. It is plausible to assume that sophisticated multienzyme complexes evolved stepwise by the association of structurally and functionally uncoupled protein subunits. The various types of TrpB proteins make the tryptophan synthase complex an excellent model to study the mechanisms underlying these processes. The members of the regular TrpB1 class of β-subunits are either fused to TrpA as found in yeast (*56*) and fungi (*57*) or form tight and permanent complexes, with dissociation constants in the nanomolar range as found in, for example, *E. coli*, *Pyrococcus furiosus* (*51*, *58*, *59*), and *T. maritima* (Figure 4B). A strong and bi-directional activation occurs both in the TrpA−TrpB1 fusion proteins and in the noncovalent TrpA−TrpB1 complexes (*53*). The only investigated representative of the TrpB2i class of β-subunits is sTrpB2i. It forms a weak and transient complex with sTrpA in which activation is uni-directional from sTrpB2i to sTrpA (Tables 1 and 2). The two characterized members of the class of β-subunits not encoded in the *trp* operon are tmTrpB2 and sTrpB2o. They do not form a detectable complex with tmTrpA and sTrpA, respectively (*34*) (Figure 2B). We suggest that tmTrpB2 and sTrpB2o represent an ancient type of β-subunit and propose a model showing how TrpB2i and TrpB1 type enzymes could have evolved from them (Figure 5). According to this model, the ancient *trp*B2 gene was duplicated, and the two resulting copies were free to evolve with different objectives. One copy remained outside the *trp* operon as *trp*B2o. It either kept an already existing function or took over a new one, for example, acting as indole salvage protein (*34*). The other copy was integrated into the operon as *trp*B2i, which resulted in its coordinated expression with the *trp*A gene and the concomitant formation of a weak and transient complex with uni-directional activation of the catalytically inefficient TrpA subunit by TrpB2i. This situation appears to have been conserved in *S. solfataricus*. Further on, TrpB2i evolved into TrpB1, which forms a tight and permanent complex with TrpA in which bi-directional activation occurs. This situation is found in *T. maritima*. Mesophilic organisms such as *E. coli*, for which TrpB2 no longer provided a selective advantage as an indole salvage protein, lost the corresponding *trp*B2 gene. Finally, the TrpB1 and TrpA genes were fused, yielding the bi-functional tryptophan synthase polypeptide

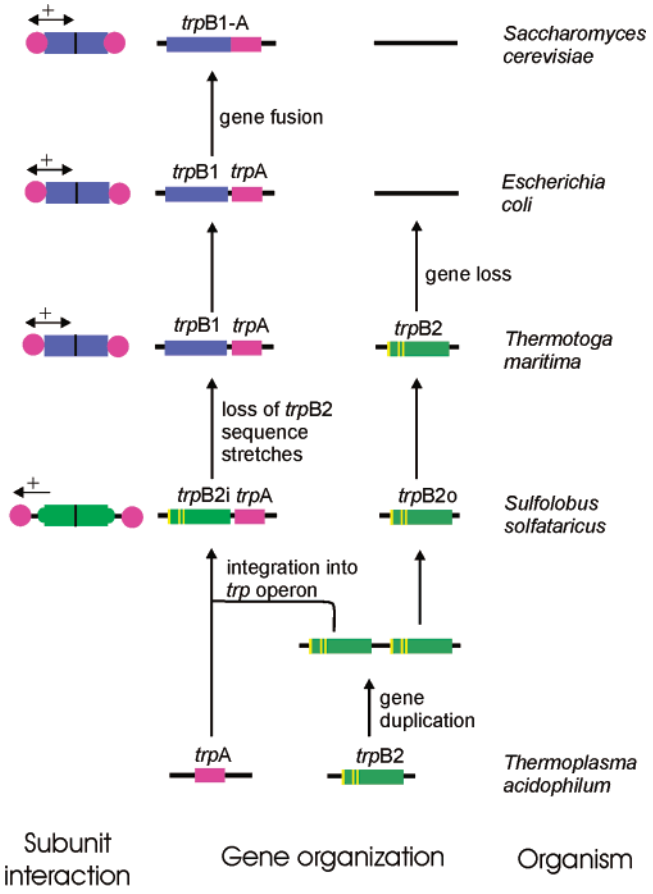

FIGURE 5: Hypothetical model for the evolution of the tryptophan synthase complex. The listed organisms provide examples of the given *trp*A and *trp*B gene organizations and the interactions between the TrpA and TrpB subunits. The horizontal arrows indicate the direction of subunit activation. The genes *trp*B2o from *S. solfataricus* and *trp*B2 from *T. maritima* might code for indole salvage proteins (*34*). It is important to note that the species shown represent specific stages of *trp*B development whose evolution might deviate from microbial speciation. See text for further details.

chain as that found in yeast. This model is further supported by the gene organization found in *Thermoplasma acidophilum*, which contains a *trp*A but no *trp*B1 gene. Its single *trp*B2 gene is located outside the *trp* operon, and a BLAST search revealed that its translated amino acid sequence is more similar to the TrpB2o than to the TrpB2i proteins of *S. solfataricus*, *S. tokodaii*, *A. pernix*, *P. aerophilum*, and *P. torridus*. We conclude that the genome of *T. acidophilum* represents an ancient *trp*B gene organization. Thus, the various types of tryptophan synthase complexes paradigmatically demonstrate how the assembly of genes in an operon can coincide with the stepwise adaptation of the gene products to a highly coordinated multi-enzyme complex (*60*). Although the model outlined in Figure 5 is based on the known *trp*A and *trp*B gene organizations and the available biochemical data of the protein products, alternative evolutionary scenarios cannot be excluded. To further test and substantiate our model, a comprehensive computational analysis including the *trp*B and *trp*A genes from all sequenced archaeal and many bacterial genomes is currently being performed. The results of this analysis will allow us to resolve in more detail the evolutionary steps that have led to the sophisticated tryptophan synthase complex found in modern organisms.

ACKNOWLEDGMENT

We thank Dr. Helmut Durchschlag for running the analytical ultracentrifuge, Dr. Rainer Merkl for sequence comparisons and stimulating discussions, and Sonja Fuchs for excellent technical assistance. We are grateful to Dr. Charles Yanofsky for helpful comments on the manuscript.

SUPPORTING INFORMATION AVAILABLE

Details of gene cloning and heterologous expression as well as protein purification. This material is available free of charge via the Internet at http://pubs.acs.org.

REFERENCES

1. Huang, X., Holden, H. M., and Raushel, F. M. (2001) Channeling of substrates and intermediates in enzyme-catalyzed reactions, *Annu. Rev. Biochem. 70*, 149−180.
2. Miles, E. W., Rhee, S., and Davies, D. R. (1999) The molecular basis of substrate channeling, *J. Biol. Chem. 274*, 12193−12196.
3. Raushel, F. M., Thoden, J. B., and Holden, H. M. (2003) Enzymes with molecular tunnels, *Acc. Chem. Res. 36*, 539−548.
4. Yanofsky, C. (2001) Advancing our knowledge in biochemistry, genetics, and microbiology through studies on tryptophan metabolism, *Annu. Rev. Biochem. 70*, 1−37.
5. Yanofsky, C. (2003) Using studies on tryptophan metabolism to answer basic biological questions, *J. Biol. Chem. 278*, 10859−10878.
6. Knöchel, T., Ivens, A., Hester, G., Gonzalez, A., Bauerle, R., Wilmanns, M., Kirschner, K., and Jansonius, J. N. (1999) The crystal structure of anthranilate synthase from *Sulfolobus solfataricus*: Functional implications, *Proc. Natl. Acad. Sci. U.S.A. 96*, 9479−9484.
7. Morollo, A. A., and Bauerle, R. (1993) Characterization of composite aminodeoxyisochorismate synthase and aminodeoxyisochorismate lyase activities of anthranilate synthase, *Proc. Natl. Acad. Sci. U.S.A. 90*, 9983−9987.
8. Morollo, A. A., and Eck, M. J. (2001) Structure of the cooperative allosteric anthranilate synthase from *Salmonella typhimurium*, *Nat. Struct. Biol. 8*, 243−247.
9. Spraggon, G., Kim, C., Nguyen-Huu, X., Yee, M. C., Yanofsky, C., and Mills, S. E. (2001) The structures of anthranilate synthase of *Serratia marcescens* crystallized in the presence of (*i*) its substrates, chorismate and glutamine, and a product, glutamate, and (*ii*) its end-product inhibitor, L-tryptophan, *Proc. Natl. Acad. Sci. U.S.A. 98*, 6021−6026.
10. Miles, E. W. (2001) Tryptophan synthase: a multienzyme complex with an intramolecular tunnel, *Chem. Rec. 1*, 140−151.
11. Hyde, C. C., Ahmed, S. A., Padlan, E. A., Miles, E. W., and Davies, D. R. (1988) Three-dimensional structure of the tryptophan synthase $\alpha_2\beta_2$ multienzyme complex from *Salmonella typhimurium*, *J. Biol. Chem. 263*, 17857−17871.
12. Dunn, M. F., Aguilar, V., Brzovic, P., Drewe, W. F., Jr., Houben, K. F., Leja, C. A., and Roy, M. (1990) The tryptophan synthase bienzyme complex transfers indole between the alpha- and beta-sites via a 25-30 A long tunnel, *Biochemistry 29*, 8598−8607.
13. Drewe, W. F., Jr., and Dunn, M. F. (1985) Detection and identification of intermediates in the reaction of L-serine with *Escherichia coli* tryptophan synthase via rapid-scanning ultraviolet-visible spectroscopy, *Biochemistry 24*, 3977−3987.
14. Kulik, V., Hartmann, E., Weyand, M., Frey, M., Gierl, A., Niks, D., Dunn, M. F., and Schlichting, I. (2005) On the structural basis of the catalytic mechanism and the regulation of the alpha subunit of tryptophan synthase from *Salmonella typhimurium* and BX1 from maize, two evolutionarily related enzymes, *J. Mol. Biol. 352*, 608−620.
15. Yamagata, Y., Ogasahara, K., Hioki, Y., Lee, S. J., Nakagawa, A., Nakamura, H., Ishida, M., Kuramitsu, S., and Yutani, K. (2001) Entropic stabilization of the tryptophan synthase α-subunit from a hyperthermophile, *Pyrococcus furiosus.* X-ray analysis and calorimetry, *J. Biol. Chem. 276*, 11062−11071.
16. Hioki, Y., Ogasahara, K., Lee, S. J., Ma, J., Ishida, M., Yamagata, Y., Matsuura, Y., Ota, M., Ikeguchi, M., Kuramitsu, S., and Yutani, K. (2004) The crystal structure of the tryptophan synthase β_2 subunit from the hyperthermophile *Pyrococcus furiosus.* Investigation of stabilization factors, *Eur. J. Biochem. 271*, 2624−2635.
17. Lee, S. J., Ogasahara, K., Ma, J., Nishio, K., Ishida, M., Yamagata, Y., Tsukihara, T., and Yutani, K. (2005) Conformational changes in the tryptophan synthase from a hyperthermophile upon $\alpha(_2)\beta(_2)$ complex formation: Crystal structure of the complex, *Biochemistry 44*, 11417−11427.
18. Kirschner, K., Lane, A. N., and Strasser, A. W. (1991) Reciprocal communication between the lyase and synthase active sites of the tryptophan synthase bienzyme complex, *Biochemistry 30*, 472−478.
19. Pan, P., and Dunn, M. F. (1996) β-Site covalent reactions trigger transitions between open and closed conformations of the tryptophan synthase bienzyme complex, *Biochemistry 35*, 5002−5013.
20. Phillips, R. S., Miles, E. W., Holtermann, G., and Goody, R. S. (2005) Hydrostatic pressure affects the conformational equilibrium of *Salmonella typhimurium* tryptophan synthase, *Biochemistry 44*, 7921−7928.
21. Rhee, S., Parris, K. D., Hyde, C. C., Ahmed, S. A., Miles, E. W., and Davies, D. R. (1997) Crystal structures of a mutant (β K87T) tryptophan synthase $\alpha 2\beta 2$ complex with ligands bound to the active sites of the α- and β-subunits reveal ligand-induced conformational changes, *Biochemistry 36*, 7664−7680.
22. Rhee, S., Miles, E. W., and Davies, D. R. (1998) Cryocrystallography of a true substrate, indole-3-glycerol phosphate, bound to a mutant (α D60N) tryptophan synthase $\alpha 2\beta 2$ complex reveals the correct orientation of active site α Glu49, *J. Biol. Chem. 273*, 8553−8555.
23. Schneider, T. R., Gerhardt, E., Lee, M., Liang, P. H., Anderson, K. S., and Schlichting, I. (1998) Loop closure and intersubunit communication in tryptophan synthase, *Biochemistry 37*, 5394−5406.
24. Weyand, M., and Schlichting, I. (1999) Crystal structure of wild-type tryptophan synthase complexed with the natural substrate indole-3-glycerol phosphate, *Biochemistry 38*, 16469−16480.
25. Weyand, M., Schlichting, I., Herde, P., Marabotti, A., and Mozzarelli, A. (2002) Crystal structure of the β $Ser^{178} \rightarrow$ Pro mutant of tryptophan synthase. A "knock-out" allosteric enzyme, *J. Biol. Chem. 277*, 10653−10660.
26. Weyand, M., and Schlichting, I. (2000) Structural basis for the impaired channeling and allosteric inter-subunit communication in the beta A169L/beta C170W mutant of tryptophan synthase, *J. Biol. Chem. 275*, 41058−41063.
27. Osborne, A., Teng, Q., Miles, E. W., and Phillips, R. S. (2003) Detection of open and closed conformations of tryptophan synthase by ^{15}N-heteronuclear single-quantum coherence nuclear magnetic resonance of bound 1-^{15}N-L-tryptophan, *J. Biol. Chem. 278*, 44083−44090.
28. Ferrari, D., Niks, D., Yang, L. H., Miles, E. W., and Dunn, M. F. (2003) Allosteric communication in the tryptophan synthase bienzyme complex: roles of the β-subunit aspartate 305-arginine 141 salt bridge, *Biochemistry 42*, 7807−7818.
29. Ferrari, D., Yang, L. H., Miles, E. W., and Dunn, M. F. (2001) Beta D305A mutant of tryptophan synthase shows strongly perturbed allosteric regulation and substrate specificity, *Biochemistry 40*, 7421−7432.
30. Raboni, S., Bettati, S., and Mozzarelli, A. (2005) Identification of the geometric requirements for allosteric communication between the α- and β-subunits of tryptophan synthase, *J. Biol. Chem. 280*, 13450−13456.
31. Kulik, V., Weyand, M., Seidel, R., Niks, D., Arac, D., Dunn, M. F., and Schlichting, I. (2002) On the role of alphaThr183 in the allosteric regulation and catalytic mechanism of tryptophan synthase, *J. Mol. Biol. 324*, 677−690.
32. Xie, G., Forst, C., Bonner, C., and Jensen, R. A. (2002) Significance of two distinct types of tryptophan synthase beta chain in Bacteria, Archaea and higher plants, *GenomeBiology 3*, RESEARCH0004.
33. Tatusov, R. L., Fedorova, N. D., Jackson, J. D., Jacobs, A. R., Kiryutin, B., Koonin, E. V., Krylov, D. M., Mazumder, R., Mekhedov, S. L., Nikolskaya, A. N., Rao, B. S., Smirnov, S., Sverdlov, A. V., Vasudevan, S., Wolf, Y. I., Yin, J. J., and Natale, D. A. (2003) The COG database: an updated version includes eukaryotes, *BMC Bioinf. 4*, 41.
34. Hettwer, S., and Sterner, R. (2002) A novel tryptophan synthase β-subunit from the hyperthermophile *Thermotoga maritima.* Quaternary structure, steady-state kinetics, and putative physiological role, *J. Biol. Chem. 277*, 8194−8201.

35. She, Q., Singh, R. K., Confalonieri, F., Zivanovic, Y., Allard, G., Awayez, M. J., Chan-Weiher, C. C., Clausen, I. G., Curtis, B. A., De Moors, A., Erauso, G., Fletcher, C., Gordon, P. M., Heikamp-de Jong, I., Jeffries, A. C., Kozera, C. J., Medina, N., Peng, X., Thi-Ngoc, H. P., Redder, P., Schenk, M. E., Theriault, C., Tolstrup, N., Charlebois, R. L., Doolittle, W. F., Duguet, M., Gaasterland, T., Garrett, R. A., Ragan, M. A., Sensen, C. W., and Van der Oost, J. (2001) The complete genome of the crenarchaeon *Sulfolobus solfataricus* P2, *Proc. Natl. Acad. Sci. U.S.A. 98*, 7835−7840.
36. Kawarabayasi, Y., Hino, Y., Horikawa, H., Jin-no, K., Takahashi, M., Sekine, M., Baba, S., Ankai, A., Kosugi, H., Hosoyama, A., Fukui, S., Nagai, Y., Nishijima, K., Otsuka, R., Nakazawa, H., Takamiya, M., Kato, Y., Yoshizawa, T., Tanaka, T., Kudoh, Y., Yamazaki, J., Kushida, N., Oguchi, A., Aoki, K., Masuda, S., Yanagii, M., Nishimura, M., Yamagishi, A., Oshima, T., and Kikuchi, H. (2001) Complete genome sequence of an aerobic thermoacidophilic crenarchaeon, *Sulfolobus tokodaii* strain7, *DNA Res. 8*, 123−140.
37. Kawarabayasi, Y., Hino, Y., Horikawa, H., Yamazaki, S., Haikawa, Y., Jin-no, K., Takahashi, M., Sekine, M., Baba, S., Ankai, A., Kosugi, H., Hosoyama, A., Fukui, S., Nagai, Y., Nishijima, K., Nakazawa, H., Takamiya, M., Masuda, S., Funahashi, T., Tanaka, T., Kudoh, Y., Yamazaki, J., Kushida, N., Oguchi, A., Kikuchi, H., and et al. (1999) Complete genome sequence of an aerobic hyper-thermophilic crenarchaeon, *Aeropyrum pernix* K1, *DNA Res. 6*, 83−101, 145−152.
38. Fitz-Gibbon, S. T., Ladner, H., Kim, U. J., Stetter, K. O., Simon, M. I., and Miller, J. H. (2002) Genome sequence of the hyperthermophilic crenarchaeon *Pyrobaculum aerophilum*, *Proc. Natl. Acad. Sci. U.S.A. 99*, 984−989.
39. Futterer, O., Angelov, A., Liesegang, H., Gottschalk, G., Schleper, C., Schepers, B., Dock, C., Antranikian, G., and Liebl, W. (2004) Genome sequence of *Picrophilus torridus* and its implications for life around pH 0, *Proc. Natl. Acad. Sci. U.S.A. 101*, 9091−9096.
40. Beismann-Driemeyer, S., and Sterner, R. (2001) Imidazole glycerol phosphate synthase from *Thermotoga maritima.* Quaternary structure, steady-state kinetics, and reaction mechanism of the bienzyme complex, *J. Biol. Chem. 276*, 20387−20396.
41. Laemmli, U. K. (1970) Cleavage of structural proteins during the assembly of the head of bacteriophage T4, *Nature 227*, 680−685.
42. Pace, C. N., Vajdos, F., Fee, L., Grimsley, G., and Gray, T. (1995) How to measure and predict the molar absorption coefficient of a protein, *Protein Sci. 4*, 2411−2423.
43. Bradford, M. M. (1976) A rapid and sensitive method for the quantitation of microgram quantities of protein utilizing the principle of protein-dye binding, *Anal. Biochem. 72*, 248−254.
44. Wales, M., Adler, F. T., and Van Holde, K. E. (1951) Sedimentation equilibria of polydisperse non-ideal solutes. VI Number-average molecular weight and molecular-weight distribution functions, *J. Phys. Colloid. Chem. 55*, 145−161.
45. Yphantis, D. A. (1964) Equilibrium ultracentrifugation of dilute solutions, *Biochemistry 3*, 297−317.
46. Creighton, T. E. (1970) A steady-state kinetic investigation of the reaction mechanism of the tryptophan synthetase of Escherichia coli, *Eur. J. Biochem. 13*, 1−10.
47. Faeder, E. J., and Hammes, G. G. (1970) Kinetic studies of tryptophan synthetase. Interaction of substrates with the B subunit, *Biochemistry 9*, 4043−4049.
48. Hommel, U., Eberhard, M., and Kirschner, K. (1995) Phosphoribosyl anthranilate isomerase catalyzes a reversible amadori reaction, *Biochemistry 34*, 5429−5439.
49. Crawford, I. P., and Ito, J. (1964) Serine deamination by the B protein of *Escherichia coli* tryptophan synthetase, *Proc. Natl. Acad. Sci. U.S.A. 51*, 390−397.
50. Eberhard, M. (1990) A set of programs for analysis of kinetic and equilibrium data, *Comput. Appl. Biosci. 6*, 213−221.
51. Creighton, T. E., and Yanofsky, C. (1966) Association of the α and β-$_2$ subunits of the tryptophan synthetase of *Escherichia coli*, *J. Biol. Chem. 241*, 980−990.
52. Xie, Y., and Reeve, J. N. (2005) Regulation of tryptophan operon expression in the archaeon *Methanothermobacter thermautotrophicus*, *J. Bacteriol. 187*, 6419−6429.
53. Miles, E. W. (1991) Structural basis for catalysis by tryptophan synthase, *Adv. Enzymol. Relat. Areas Mol. Biol. 64*, 93−172.
54. Roux, B., and Walsh, C. T. (1992) p-Aminobenzoate synthesis in *Escherichia coli*: kinetic and mechanistic characterization of the amidotransferase PabA, *Biochemistry 31*, 6904−6910.
55. Rudolph, J., and Stubbe, J. (1995) Investigation of the mechanism of phosphoribosylamine transfer from glutamine phosphoribosylpyrophosphate amidotransferase to glycinamide ribonucleotide synthetase, *Biochemistry 34*, 2241−2250.
56. Zalkin, H., and Yanofsky, C. (1982) Yeast gene TRP5: structure, function, regulation, *J. Biol. Chem. 257*, 1491−1500.
57. Burns, D. M., Horn, V., Paluh, J., and Yanofsky, C. (1990) Evolution of the tryptophan synthetase of fungi. Analysis of experimentally fused *Escherichia col*i tryptophan synthetase alpha and beta chains, *J. Biol. Chem. 265*, 2060−2069.
58. Lane, A. N., Paul, C. H., and Kirschner, K. (1984) The mechanism of self-assembly of the multi-enzyme complex tryptophan synthase from *Escherichia coli*, *EMBO J. 3*, 279−287.
59. Ogasahara, K., Ishida, M., and Yutani, K. (2003) Stimulated interaction between α and β subunits of tryptophan synthase from hyperthermophile enhances its thermal stability, *J. Biol. Chem. 278*, 8922−8928.
60. Dandekar, T., Snel, B., Huynen, M., and Bork, P. (1998) Conservation of gene order: a fingerprint of proteins that physically interact, *Trends Biochem. Sci. 23*, 324−328.
61. Notredame, C., Higgins, G. D., and Heringa, J. (2000) T-Coffee: A novel method for fast and accurate multiple sequence alignment, *J. Mol. Biol. 302*, 205−217.

BI061684B